

Tandem Duplication Producing a Novel Oncogenic *BRAF* Fusion Gene Defines the Majority of Pilocytic Astrocytomas

David T.W. Jones,¹ Sylvia Kocialkowski,¹ Lu Liu,¹ Danita M. Pearson,¹ L. Magnus Bäcklund,² Koichi Ichimura,¹ and V. Peter Collins¹

¹Division of Molecular Histopathology, Department of Pathology, University of Cambridge, Cambridge, United Kingdom and ²Department of Oncology-Pathology, Karolinska Hospital, Stockholm, Sweden

Abstract

Brain tumors are the most common solid tumors of childhood, and pilocytic astrocytomas (PA) are the most common central nervous system tumor in 5 to 19 year olds. Little is known about the genetic alterations underlying their development. Here, we describe a tandem duplication of ~2 Mb at 7q34 occurring in 66% of PAs. This rearrangement, which was not observed in a series of 244 higher-grade astrocytomas, results in an in-frame fusion gene incorporating the kinase domain of the *BRAF* oncogene. We further show that the resulting fusion protein has constitutive BRAF kinase activity and is able to transform NIH3T3 cells. This is the first report of *BRAF* activation through rearrangement as a frequent feature in a sporadic tumor. The frequency and specificity of this change underline its potential both as a therapeutic target and as a diagnostic tool. [Cancer Res 2008;68(21):8673–7]

Introduction

Pilocytic astrocytomas (PA) are the most common pediatric brain tumor, with peak incidence in the first decade of life (1). They are not usually infiltrating, with malignancy grade 1 in the WHO classification (2), and progression to higher grades is extremely rare. Although gross total resection may result in a cure, recurrence is seen in up to 19% of cases (3), and both the initial tumor and subsequent treatment are associated with considerable morbidity.

Classic histology includes bipolar tumor cells, eosinophilic Rosenthal fibers, and granular bodies alternating with microcystic areas comprising loosely arranged astrocyte-like cells. However, PAs can show a wide morphologic spectrum, with areas resembling oligodendroglioma or higher-grade astrocytoma. Necrosis, vascular proliferation, and mitotic figures do not have the same significance as in other gliomas (2), and definitive histologic diagnosis can be challenging. This is particularly important when considering the treatment modalities used to combat PAs (usually surgery with careful follow-up) versus most other gliomas (generally surgery followed by radiotherapy and chemotherapy).

Little is known about the molecular mechanisms involved in the tumorigenesis of PAs. Cytogenetic and array-based studies have indicated grossly normal genetic complements in most cases, with whole chromosomal gains, particularly of chromosomes 5 and 7, observed in some (e.g., refs. 4, 5). Two recent studies have reported recurrent gains at 7q34 in PAs. The first concludes that this leads to

gain of *BRAF*, with subsequent BRAF overexpression (6). The second reports *HIPK2* as the target for amplification and overexpression (7). However, our data show that tandem duplication at this locus produces a novel oncogenic fusion gene incorporating a constitutively active BRAF kinase domain. This is the first report of a common, specific genetic alteration underlying the formation of PAs. The frequency and specificity of this change underline its potential both as a therapeutic target and as a diagnostic marker.

Materials and Methods

Patients, DNA, RNA, and microarray analysis. Clinicopathologic data are given in Supplementary Table S1. Nucleic acid extraction and the whole-genome microarray have been described previously (5), and the array data have been deposited in Gene Expression Omnibus (GEO; accession number GSE11263). A tiling-path array with overlapping clones covering >92% of chromosome 7 was constructed as per the whole-genome array. Clones were obtained from the Wellcome Trust Sanger Institute (Hinxton, United Kingdom). These data have also been deposited with GEO (accession number GSE11265). An oligonucleotide array covering the ends of the duplicated region was constructed by Oxford Gene Technologies Ltd. Hybridizations and data extraction for this array were performed by the manufacturer.

5' Rapid amplification of cDNA ends, mutation screening, PCR, and sequencing. 5' Rapid amplification of cDNA ends (RACE) was carried out with a RNA ligase-mediated kit (Invitrogen) as per the manufacturer's instructions, with nested reverse primers (PC4588 and PC4590) toward the start of the known reference sequence. Primer sequences and conditions for PCRs are described in Supplementary Table S2. Cycle sequencing was performed with BigDye v3.1 chemistry and run on a 3100-Avant Genetic Analyzer (Applied Biosystems).

Cloning and expression constructs. Full open reading frames for long- and short-form KIAA1549:BRAF transcripts ($K^{Ex16}B^{Ex9}$) as well as wild-type and V600E-mutant BRAF were cloned into a pCR4 vector using a TA Cloning kit (Invitrogen). These constructs were used as templates for the addition of COOH-terminal hemagglutinin (HA) tags and subsequent cloning into expression vectors. A pcDNA3.1-based vector (Invitrogen) was used for the kinase assay. A pBABE-puro vector (a kind gift from Dr. S. Turner, University of Cambridge) was used for stable transductions.

Cell culture. Cos-7 (CRUK Cell Services) and Phoenix cells (a kind gift from Dr. S. Turner) were grown in 5% CO₂ in high-glucose DMEM (PAA Laboratories Ltd.) supplemented with 10% fetal bovine serum (FBS; PAA Laboratories). For NIH3T3 cells (a kind gift from Professor Y. Yuasa, Tokyo Medical and Dental University, Tokyo, Japan), 10% calf serum (PAA Laboratories) was used in place of FBS. Cells were grown at 37°C unless otherwise stated.

Kinase assay. HA-tagged I-KIAA1549:BRAF, s-KIAA1549:BRAF, BRAF^{WT}, and BRAF^{V600E} were transfected into Cos-7 cells using Lipofectamine 2000 (Invitrogen). Cells were harvested in radioimmunoprecipitation assay buffer supplemented with Complete Protease Inhibitor Cocktail (Roche Applied Science). Tagged protein was purified with an anti-HA immunoprecipitation kit (Sigma-Aldrich). BRAF kinase activity was determined with a

Note: Supplementary data for this article are available at Cancer Research Online (<http://cancerres.aacrjournals.org/>).

Requests for reprints: David Jones, Division of Molecular Histopathology, Level 3 Lab Block, Box 231, Addenbrooke's Hospital, Cambridge CB2 0QQ, United Kingdom. Phone: 44-122-376-2084; Fax: 44-122-358-6670; E-mail: davidjones@cantab.net.

©2008 American Association for Cancer Research.
doi:10.1158/0008-5472.CAN-08-2097

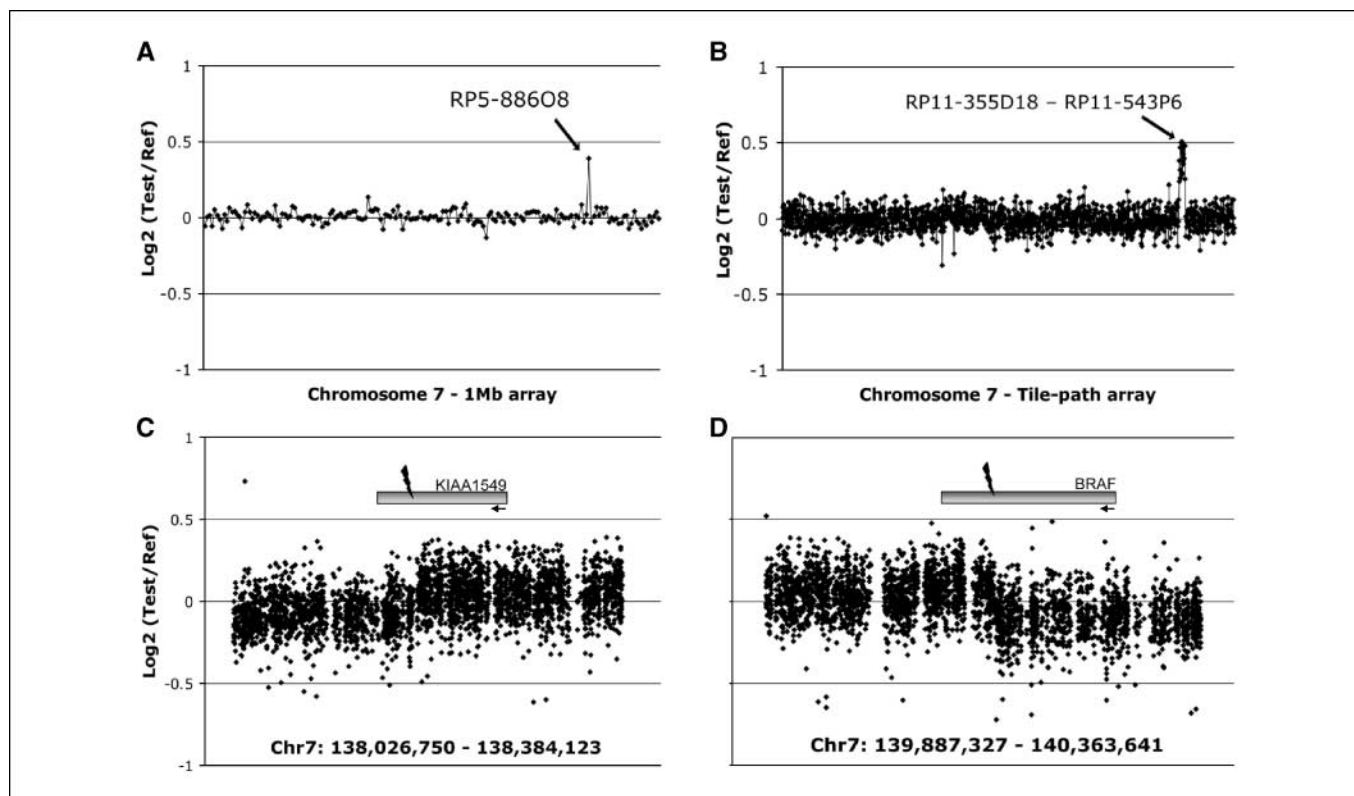


Figure 1. Identification of copy number gain at 7q34 in PAs. *A*, a representative 1-Mb array plot from PA2 showing gain of clone RP5-886O8 at 7q34. *B*, a chromosome 7 tiling-path array plot from the same tumor, showing gain of ~2 Mb spanning 22 clones between RP11-355D18 and RP11-543P6. *C* and *D*, a custom oligonucleotide array covering the ends of the region of gain, showing a change in copy number within the *KIAA1549* and *BRAF* genes.

chemiluminescent kinase assay kit (Millipore UK Ltd.). Kinase activity was normalized for input protein quantity as assessed by blotting with an antibody against BRAF COOH terminus (C-19; Santa Cruz Biotechnology). Western blots were visualized with ECL+ reagent (GE Healthcare) using a Fujifilm LAS-4000 imager and quantified with AIDA analysis software (Fujifilm UK Ltd.).

Soft agar assay. A viral packaging line (Phoenix) was transfected with s-KIAA1549:BRAF, BRAF^{WT}, BRAF^{V600E}, Ras^{V12}, and empty pBABE-puro vector using FuGene 6 reagent (Roche Applied Science) with 4 μ g plasmid and 2 μ g helper phage per 10-cm dish. At 24 h after transfection, cells were transferred to 32°C. Forty-eight hours after transfection, supernatant was collected and filtered through a 45- μ m filter before being overlaid onto NIH3T3 cells. Twenty-four hours after infection, medium was changed and cells moved back to 37°C. Mass selection with 2 μ g/mL puromycin (Sigma-Aldrich) was applied at 48 h after infection. Resistant cells were harvested, and 1×10^4 were mixed with 2 mL of 0.35% agarose in complete medium and overlaid onto 2 mL of 0.6% agarose in a six-well plate. A further overlay of 2 mL complete medium was changed every 72 h. Cell growth was examined at 11 d after plating.

Statistical analysis. Equality of survival distributions by fusion gene status was assessed by a log-rank test using Statistical Package for the Social Sciences version 15 (SPSS, Inc.).

Results

Microarray copy number analysis reveals a recurrent region of gain at 7q34 in PAs. A series of 44 well-documented PAs (no pilomyxoid variants) were investigated using large-insert clone microarrays. Clinicopathologic details are given in Supplementary Table S1. Large-scale changes observed on the 1-Mb whole-genome array have been described previously (5). A chromosome 7 tiling-

path array was used to validate a recurrent change observed on the 1-Mb array (Fig. 1A). Our analysis revealed a region of gain of ~2 Mb within 7q34, between clones RP11-355D18 and RP11-543P6, in 29 of 44 cases (66%; Fig. 1B). Analysis of a subset of matched blood samples with the same platform eliminated the possibility of either a copy number polymorphism or a germ-line alteration (data not shown). The tumor microarray data have been deposited in the National Center for Biotechnology Information GEO³ (accession numbers GSE11263 and GSE11265).

Tandem duplication at 7q34 produces a novel fusion gene. The location of the gain as a tandem duplication was shown by interphase fluorescence *in situ* hybridization (FISH; Supplementary Fig. S1). To determine the ends of the duplication, a custom oligonucleotide array covering the breakpoints was constructed. This indicated a break in intron 16 of the uncharacterized gene *KIAA1549* and intron 8 of *BRAF* (Fig. 1C and D). *KIAA1549* exons are numbered according to accession number AM989467 in the European Molecular Biology Laboratory (EMBL) Nucleotide Sequence Database.⁴ The rearrangement is shown schematically in Fig. 2A. Reverse transcription-PCR (RT-PCR) with primers in exon 16 of *KIAA1549* (PC4578) and exon 9 of *BRAF* (PC4579) gave the predicted product in many tumors, but not in all cases, showing gain at 7q34 by microarray analysis. Primers in more distal exons (PC4644 and PC4645) revealed three mRNA breakpoints

³ <http://www.ncbi.nlm.nih.gov/geo/>

⁴ <http://www.ebi.ac.uk/embl/>

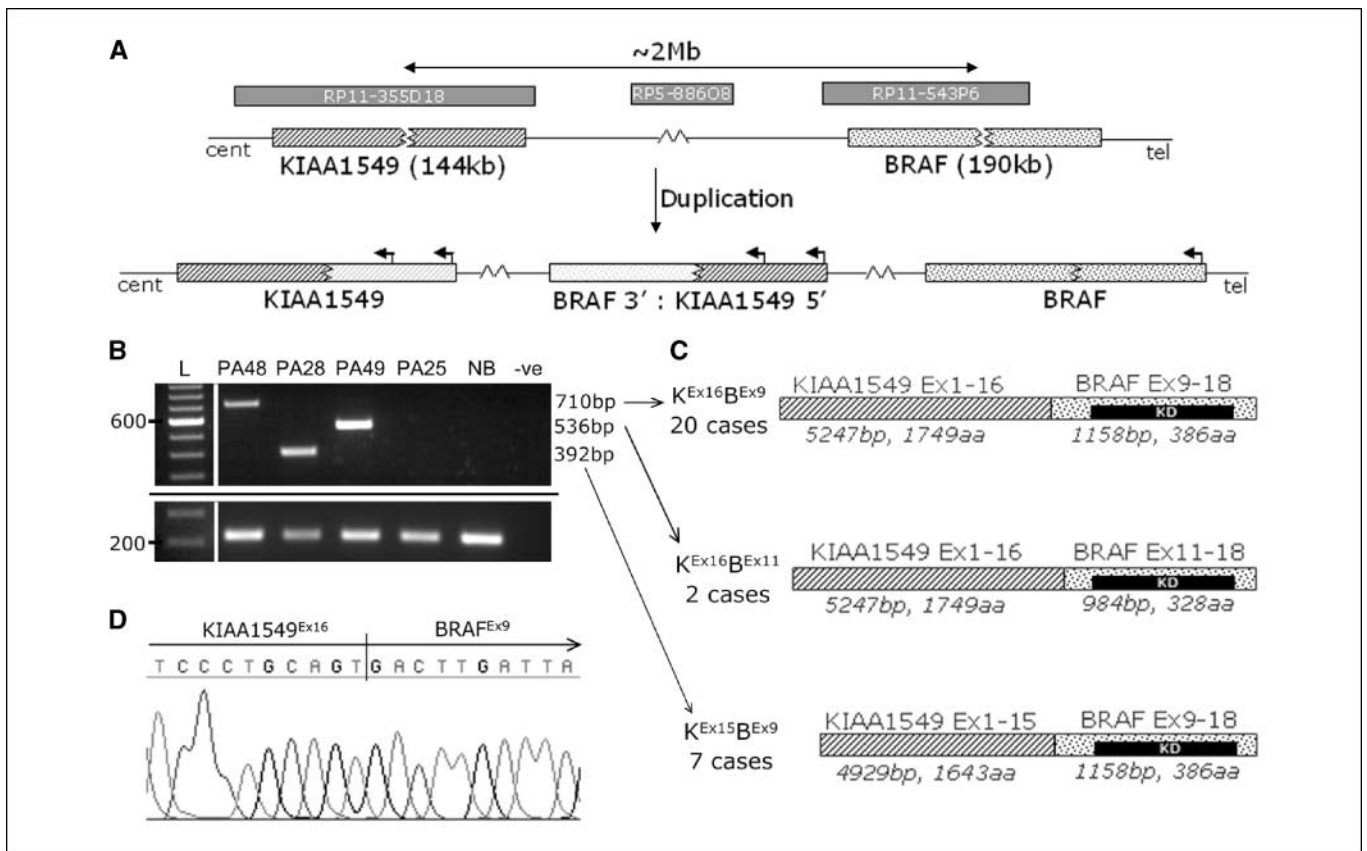


Figure 2. Tandem duplication at 7q34 produces a fusion gene between *KIAA1549* and *BRAF*. *A*, a schematic diagram of the tandem duplication event observed at 7q34. Clones flanking the region of gain and the 1-Mb clone from the region are indicated. FISH analysis confirmed a tandem duplication (see Supplementary Fig. S1). *B*, RT-PCR analysis with primers in *KIAA1549* exon 15 (PC4645) and *BRAF* exon 11 (PC4644) showing the three different mRNA fusion junctions observed (top) and a control locus in wild-type *BRAF* exons (bottom; expected product, 214 bp). PA25 does not harbor the 7q34 gain. PCR products were electrophoresed on a 1.5% agarose gel and visualized on a UV transilluminator (UVP Ltd.). *L*, 100-bp DNA size ladder (Invitrogen); *NB*, normal brain cDNA (Ambion); *-ve*, no template control. *C*, a schematic of the mRNA/proteins formed by the three different fusion products, and their frequency in our series. All three retain intact open reading frames. *KD*, *BRAF* kinase domain. *D*, a sequence trace confirming a fusion between *KIAA1549* exon 16 and *BRAF* exon 9.

occurring with varying frequency (Fig. 2*B* and *C*). RT-PCR confirmed the presence of a fusion transcript in all cases where 7q34 duplication was indicated by the microarrays. The most common fusion was between *KIAA1549* exon 16 and *BRAF* exon 9 ($K^{Ex16}B^{Ex9}$; 20 cases) followed by *KIAA1549* exon 15 and *BRAF* exon 9 ($K^{Ex15}B^{Ex9}$; 7 cases) and *KIAA1549* exon 16 and *BRAF* exon 11 ($K^{Ex16}B^{Ex11}$; 2 cases). RT-PCR products were sequenced for confirmation and verified retention of an open reading frame in all fusion transcripts (Fig. 2*D*; data not shown).

Identification of full-length *KIAA1549* and an internal promoter producing a shorter isoform. To clone the *KIAA1549*:*BRAF* fusion gene, it was necessary to determine the true 5' end of *KIAA1549* because previously documented sequences (e.g., Ensembl transcript ENST00000242365)⁵ suggested 5' truncation. 5' RACE analysis revealed an additional exon ~60 kb upstream of the previously documented *KIAA1549* exon 1. This exon was located in an Ensembl-annotated CpG island with a transcriptional start site (TSS) predicted by the Eponine TSS finder

(8), and contains two start AUG codons in frame with exon 2. The new first intron has canonical GT/AG splice donor/acceptor sites.

In addition to this, Genbank sequence XM_935390 indicated the existence of a shorter *KIAA1549* transcript originating from a promoter within intron 8, with a start codon in this intronic sequence. Shorter forms of both wild-type *KIAA1549* (*s-KIAA1549*) and *KIAA1549*:*BRAF* fusions were confirmed by RT-PCR (data not shown). The presence of stop codons in all three reading frames in the 5' untranslated region of the short form excludes the possibility of it being a rare splice variant of the longer form. Furthermore, an alternative splice acceptor site in intron 19 gives two variants of *KIAA1549* exon 20 (ex20b being 48 bp longer than ex20a). Sequences of long- and short-form wild-type *KIAA1549* variants and *KIAA1549*:*BRAF* fusion transcripts have been deposited in the EMBL database, as described in Supplementary Table S3.

The novel *BRAF* fusion gene shows constitutive kinase activity and transforms NIH3T3 cells. The full coding sequence of the long (*l*-) and short (*s*-) forms of the most common *KIAA1549*:*BRAF* fusion ($K^{Ex16}B^{Ex9}$), a constitutively active mutant *BRAF* (V600E), and wild-type *BRAF* were cloned and used to transfect Cos-7 cells. The common $K^{Ex16}B^{Ex9}$ fusion was taken to be representative of *KIAA1549*:*BRAF* fusion as a whole. The breakpoint variants are expected to be functionally similar because they

⁵ <http://www.ensembl.org>

all possess an in-frame BRAF kinase domain with a substituted NH₂ terminus lacking the BRAF autoregulatory domain (see Discussion). Both isoforms of the fusion protein showed constitutive kinase activity at levels similar to or higher than BRAF^{V600E} (Fig. 3A). NIH3T3 cells were then stably transduced with either empty pBABE-puro vector, HRas^{V12}, BRAF^{V600E}, or s-K^{Ex16BEx9}. Cells with the fusion construct displayed anchorage-independent growth in soft agarose (Fig. 3B), showing its transforming potential in this model system.

Gain at 7q34 is highly specific for PA. This 7q34 duplication seems to be highly specific for PA. Gain of clone RP5-886O8 on the 1-Mb array was seen in 29 of 29 PAs known to harbor the ~2-Mb duplication (Fig. 1A) and was therefore considered an accurate marker of gain at this locus. RP5-886O8 gain was not observed in any of 60 anaplastic astrocytomas or 184 glioblastomas (data not shown). Screening of 22 grade 2 astrocytomas and 96 oligodendroglial or mixed astrocytic/oligodendroglial tumors showed 6 of these to have gain at 7q34, confirmed by tiling-path array analysis (data not shown). These cases are all children or young adults with posterior fossa lesions and extremely long survival (all >12 years; see Supplementary Table S4). It is thus likely that these six tumors represent PAs that were originally diagnosed otherwise. However, even if these cases are not PAs, they are biologically benign gliomas, and the specificity of the change is still excellent (6 false positives from 406 cases; specificity, 98.5%), highlighting its potential use as a molecular diagnostic marker.

The effect of KIAA1549:BRAF on survival. The effect of the fusion gene on survival was examined. At last follow-up (September 2006), data were available on 37 of 44 cases and 35 were still alive (average follow-up, 150 months; range, 105–215 months). The two deaths occurred 5 and 167 months postoperatively (cause unknown). The tumors from the deceased patients both showed 7q34 gain. However, there was no significant difference in survival at latest follow-up with respect to the presence of the KIAA1549:BRAF fusion (overall survival, 91% versus 100%, respectively; $P = 0.26$, log-rank test).

Mutational analysis of BRAF and H-RAS, K-RAS, and N-RAS. Three individual cases of PA with a mutation in KRAS have previously been reported (9–11), and a recent report showed BRAF mutation in 3 of 53 cases (6%; ref. 6). Tumors not showing 7q34 gain were screened for point mutations in BRAF (exons 11 and 15) and H-RAS, K-RAS, and N-RAS (exons 2 and 3) by PCR amplification and direct sequencing. Two cases (PA7 and PA25) showed a valine-to-glutamate substitution at codon 600 (BRAF^{V600E}), a known mutational hotspot (data not shown). No mutations were observed in the RAS genes.

Discussion

Our results show a tandem duplication at 7q34 leading to a fusion between KIAA1549 and BRAF in 66% of PAs. Three different fusion breakpoints are observed, but all retain an open reading frame encoding the BRAF kinase domain, in a situation analogous to that of the BCR/ABL fusion. A recent report describes 11 tandem duplications in two cancer cell lines, suggesting that this class of rearrangement may be more common than previously thought (12). Our data indicate that reevaluation of single-copy gains seen in other tumors may therefore be warranted, and further highlight the importance of activating gene rearrangements in solid tumors.

NH₂-terminal truncation of BRAF through deletion or rearrangement leads to constitutive kinase activity (13) because the activity of wild-type BRAF is regulated by interaction of its autoregulatory

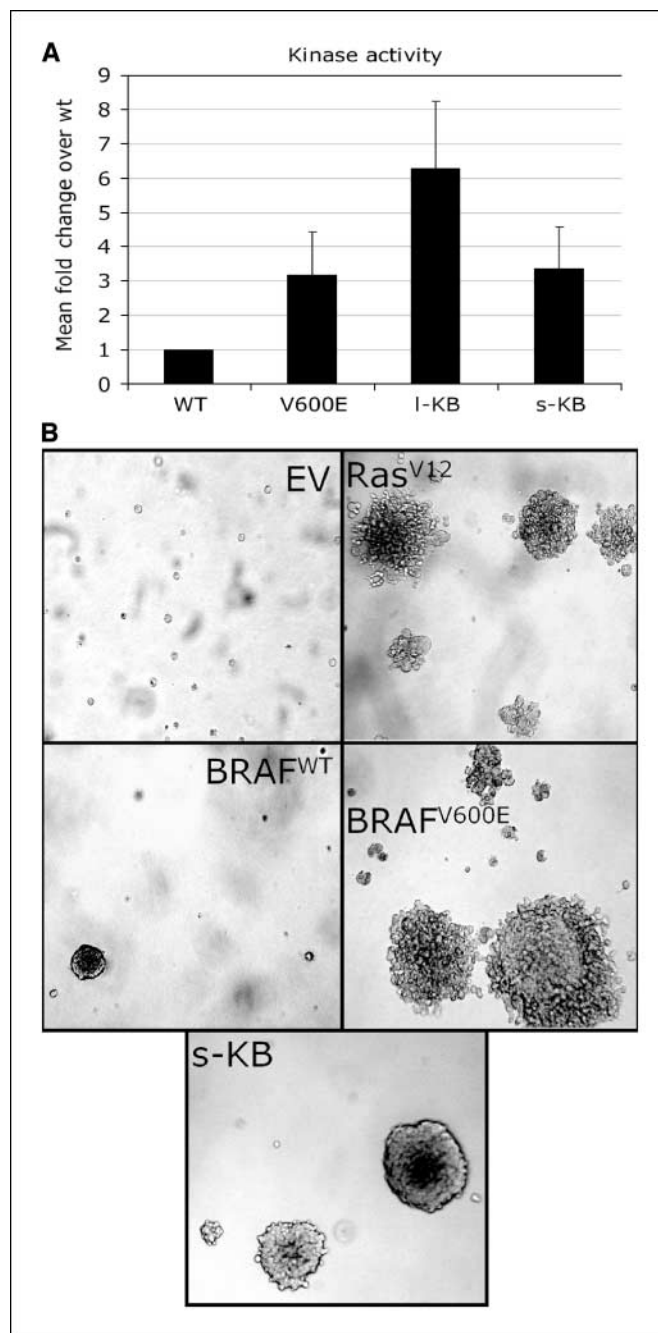


Figure 3. The KIAA1549:BRAF fusion gene shows constitutive kinase activity and transforms NIH3T3 cells. *A*, an *in vitro* BRAF kinase activity assay showing the fusion proteins to have constitutive kinase activity at a level similar to or higher than that of mutant BRAF. WT, wild-type BRAF; V600E, BRAF^{V600E}; I-KB, long-form KIAA1549-BRAF (K^{Ex16BEx9}) fusion; s-KB, short-form KIAA1549-BRAF (K^{Ex16BEx9}) fusion. Columns, fold increase in activity over wild-type, averaged over triplicate assays; bars, SD. Two independent transfections gave similar results. *B*, NIH3T3 cells transduced with pBABE-puro vector alone (EV), HRas^{V12} (Ras^{V12}), wild-type BRAF (WT), BRAF^{V600E}, or short-form KIAA1549-BRAF (K^{Ex16BEx9}) fusion (s-KB) were grown in soft agarose. Active RAS, mutant BRAF, and the fusion protein all display anchorage-independent growth. Photos shown are representative fields taken at 11 d after plating.

NH₂-terminal region, including the Ras-binding domain, with the kinase domain (14). Oncogenic activation of BRAF is well documented in many tumors (15). However, this usually results from point mutation rather than gene rearrangement, with a

hotspot at residue 600 (BRAF^{V600E}).⁶ An activating rearrangement of *BRAF* in a primary tumor was first reported in four papillary thyroid carcinomas, where an *AKAP9:BRAF* fusion was described in short-latency, post-Chernobyl tumors (13). Translocations involving *BRAF* have also been reported in two cases of large congenital melanocytic nevi (16). The present findings are thus unique in reporting *BRAF* activation through rearrangement as a common feature of a sporadic tumor.

Recent reports have shown that constitutive activation of BRAF can lead to oncogene-induced senescence (OIS) in benign tumors (17). Thus, OIS may contribute to the benign course and slow growth of PAs. The role of activated BRAF in regulating the mitotic spindle checkpoint is also of interest in light of reports of aneuploidy in PAs (5, 18).

The importance of RAS/RAF signaling in PAs is further supported by the increased incidence of PAs in neurofibromatosis type 1 (NF1). Mutations of the *NF1* gene in this syndrome lead to hyperactive RAS signaling and RAF activation (19). Three tumors in our series (PA19, PA41, and PA42) were diagnosed as having clinical features of NF1. None of these possessed the *KIAA1549:BRAF* fusion, suggesting that only one "hit" on the mitogen-activated protein kinase pathway is required for PA development. The total number of cases with an identified alteration in this pathway in our series is 34 of 44 (77%; see Supplementary Table S1).

The identification of a recurrent, transforming genetic event in the majority of PAs represents a significant increase in our

understanding of this entity. The *KIAA1549:BRAF* fusion is seen across all ages and in various locations in our series, including the cerebellum, ventricles, hypothalamus, and optic nerve. This is in contrast with previous reports suggesting differences in genomic and/or expression signatures with respect to age and tumor location (5, 20) and may suggest a precursor cell common to most cases of PA that displays a degree of oncogene tropism.

In conclusion, due to the frequency and transforming activity of the recurrent fusion event presented here, we consider it likely that this is the initiating lesion in the majority of PAs. The prevalence and specificity of this change strongly indicate potential uses both as a diagnostic marker and in a targeted therapeutic setting.

Disclosure of Potential Conflicts of Interest

No potential conflicts of interest were disclosed.

Acknowledgments

Received 6/3/2008; revised 7/31/2008; accepted 8/26/2008.

Grant support: Samantha Dickson Brain Tumour Trust, Cancer Research UK, Jacqueline Seroussi Memorial Foundation for Cancer Research, and Cambridge Fund for the Prevention of Disease.

The costs of publication of this article were defrayed in part by the payment of page charges. This article must therefore be hereby marked *advertisement* in accordance with 18 U.S.C. Section 1734 solely to indicate this fact.

We thank Dr. M.G. McCabe, Dr. M. Dimitriadi, R. Chan, A. Goatly, S. Rigby, F. McDuff, Dr. S. Turner, and Professor Y. Yuasa for help and for reagents and the Mapping Core, Map Finishing, and Microarray Facility groups of the Wellcome Trust Sanger Institute and the Centre for Microarray Resources in the Department of Pathology, University of Cambridge for assistance.

⁶ <http://www.sanger.ac.uk/genetics/CGP/cosmic/>

References

1. Central Brain Tumor Registry of the United States. Statistical report: primary brain tumors in the United States, 1998-2002. Chicago (IL): CBTRUS; 2006.
2. Louis DN, Ohgaki H, Wiestler OD, Cavenee WK. WHO classification of tumours of the central nervous system. Lyon (France): IARC Press; 2007.
3. Dirven CM, Mooij JJ, Molenaar WM. Cerebellar pilocytic astrocytoma: a treatment protocol based upon analysis of 73 cases and a review of the literature. *Childs Nerv Syst* 1997;13:17-23.
4. Zattara-Cannoni H, Gambarelli D, Lena G, et al. Are juvenile pilocytic astrocytomas benign tumors? A cytogenetic study in 24 cases. *Cancer Genet Cytogenet* 1998; 104:157-60.
5. Jones DT, Ichimura K, Liu L, Pearson DM, Plant K, Collins VP. Genomic analysis of pilocytic astrocytomas at 0.97 Mb resolution shows an increasing tendency toward chromosomal copy number change with age. *J Neuropathol Exp Neurol* 2006;65:1049-58.
6. Pfister S, Janzarik WG, Remke M, et al. BRAF gene duplication constitutes a mechanism of MAPK pathway activation in low-grade astrocytomas. *J Clin Invest* 2008; 118:1739-49.
7. Deshmukh H, Yeh TH, Yu J, et al. High-resolution, dual-platform aCGH analysis reveals frequent HIPK2 amplification and increased expression in pilocytic astrocytomas. *Oncogene* 2008;27:4745-51.
8. Down TA, Hubbard TJ. Computational detection and location of transcription start sites in mammalian genomic DNA. *Genome Res* 2002;12:458-61.
9. Janzarik WG, Kratz CP, Loges NT, et al. Further evidence for a somatic KRAS mutation in a pilocytic astrocytoma. *Neuropediatrics* 2007;38:61-3.
10. Maltzman TH, Mueller BA, Schroeder J, et al. Ras oncogene mutations in childhood brain tumors. *Cancer Epidemiol Biomarkers Prev* 1997;6:239-43.
11. Sharma MK, Zehnbauser BA, Watson MA, Gutmann DH. RAS pathway activation and an oncogenic RAS mutation in sporadic pilocytic astrocytoma. *Neurology* 2005;65:1335-6.
12. Campbell PJ, Stephens PJ, Pleasance ED, et al. Identification of somatically acquired rearrangements in cancer using genome-wide massively parallel paired-end sequencing. *Nat Genet* 2008;40:722-9.
13. Ciampi R, Knauf JA, Kerler R, et al. Oncogenic AKAP9-BRAF fusion is a novel mechanism of MAPK pathway activation in thyroid cancer. *J Clin Invest* 2005;115:94-101.
14. Tran NH, Wu X, Frost JA. B-Raf and Raf-1 are regulated by distinct autoregulatory mechanisms. *J Biol Chem* 2005;280:16244-53.
15. Davies H, Bignell GR, Cox C, et al. Mutations of the BRAF gene in human cancer. *Nature* 2002;417: 949-54.
16. Dessars B, De Raeve LE, El Housni H, et al. Chromosomal translocations as a mechanism of BRAF activation in two cases of large congenital melanocytic nevi. *J Invest Dermatol* 2007;127:1468-70.
17. Michaloglou C, Vredeveld LC, Soengas MS, et al. BRAF600-associated senescence-like cell cycle arrest of human naevi. *Nature* 2005;436:720-4.
18. Cui Y, Guadagno TM. B-Raf(V600E) signaling deregulates the mitotic spindle checkpoint through stabilizing Mps1 levels in melanoma cells. *Oncogene* 2008;27: 3122-33.
19. Le LQ, Parada LF. Tumor microenvironment and neurofibromatosis type I: connecting the GAPS. *Oncogene* 2007;26:4609-16.
20. Sharma MK, Mansur DB, Reifenberger G, et al. Distinct genetic signatures among pilocytic astrocytomas relate to their brain region origin. *Cancer Res* 2007; 67:890-900.